

Electronic Supplementary Material

Adaptive zones shape the magnitude of premating isolation in *Timema* stick insects
*Moritz Muschick¹**, *Victor Soria-Carrasco²**, *Jeffrey L. Feder*, *Zach Gompert*, and *Patrik Nosil*

*These authors contributed equally to this work.

Contact: ¹moritz.muschick@eawag.ch; ²victor.soria-carrasco@jic.ac.uk

Table S1. Populations used in this work for transition rate analyses and host preference experiments. (csv file)

Table S2. Host preference experiments. See Table S1 for correspondence between host plant codes and host plant genera. (csv file)

Table S3. Phylogenetic hypotheses testing. We used two datasets: using strictly variant sites with ascertainment bias substitution models for inference ('strict-ASC') and including also sites with ambiguities and using substitution standard models for inference ('relaxed'). We tested five hypotheses: clustering by division ('division', implies a single shift between conifers and flowering plants), clustering by species ('species'), clustering by species and division within species ('division within species', minimizes the number of shifts within species), Bayesian inference from Riesch *et al.* (2017) ('BEAST'), and maximum-likelihood tree inferred with IQTREE ('free'). We used IQTREE and consel to estimate p-values of Shimodaira-Hasegawa (p-SH), weighted Shimodaira-Hasegawa (p-WSH) and Approximately Unbiased (p-AU) test. The hypotheses rejected are highlighted using bold text.

Dataset	No sites	Program	Hypothesis	p-SH	p-WSH	p-AU
strict-ASC	5797	IQTREE	Division	0.000	0.000	0.000
			Species	0.771	0.661	0.321
			division within species	0.008	0.000	0.000
			BEAST	1.000	0.912	0.576
			Free	0.919	0.917	0.566
		consel	Division	0.000	0.000	0.000
			Species	0.779	0.684	0.345
			division within species	0.007	0.000	0.000
			BEAST	0.917	0.912	0.546
			Free	0.911	0.915	0.576
Relaxed	19556	IQTREE	Division	0.000	0.000	0.000
			Species	0.776	0.653	0.311
			division within species	0.030	0.000	0.000
			BEAST	0.912	0.912	0.573
			Free	1.000	0.921	0.579
		consel	Division	0.000	0.000	0.000
			Species	0.775	0.660	0.314
			division within species	0.018	0.000	0.000
			BEAST	0.903	0.855	0.494
			Free	0.926	0.951	0.646

Table S4. Transition rate models support. Each model was fit to 1000 trees from the posterior distribution of time calibrated trees (from Riesch *et al.* 2017) using two methods: joint and marginal and five different root probabilities: same probability for all host genera ('flat'), root probabilities following Yang (2006) ('yang'), root probabilities estimated following Maddison *et al.* (2007) and FitzJohn *et al.* (2009) ('madd'), same probability for all conifer host genera ('con'), and same probability for all flowering plant genera ('flo'). (csv file)

Table S5. Transition rate estimates for all models (methods and root probabilities as in Table S4). (csv file)

Table S6. Analysis of divergence between pairs of *Timema* population in host preference.

	Predicted mean (model error) preference difference	Estimate (logit)	Std. Error	z-value	Pr(> z)
Both flowering plant hosts	One conifer and one flowering plant host				
1) all pairs (n=24 pairs)					
Intercept					
Host use divergence	0.22 (0.15)	0.48 (0.18)	1.1539	0.3294	3.5035 0.0005
2) within-species pairs (n=18 pairs)					
Intercept					
Host use divergence	0.23 (0.16)	0.60 (0.19)	1.6260	0.5979	2.7197 0.0065
3) within-species, same locality pairs (n=13 pairs)					
Intercept					
Host use divergence	0.22 (0.17)	0.60 (0.20)	1.6555	0.6651	2.4890 0.0128

Figure S1. Support for each model using different root probabilities and either joint estimation of transition rates and ancestral states (A-E) or marginal estimation of rates followed by ancestral state estimation (F-J) (see main text and Fig. 3 for details on models and root priors). Violin plots depict the distribution of ΔAICc values (difference in sample-size corrected AIC between the focal model and the best model) after fitting the models by maximum likelihood to 1000 trees randomly taken from the posterior distribution from Riesch *et al.* (2017).

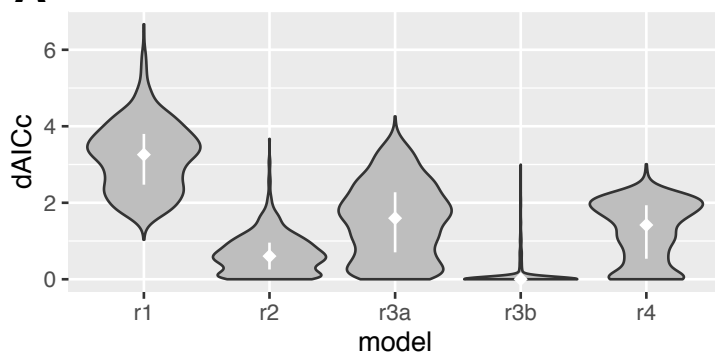
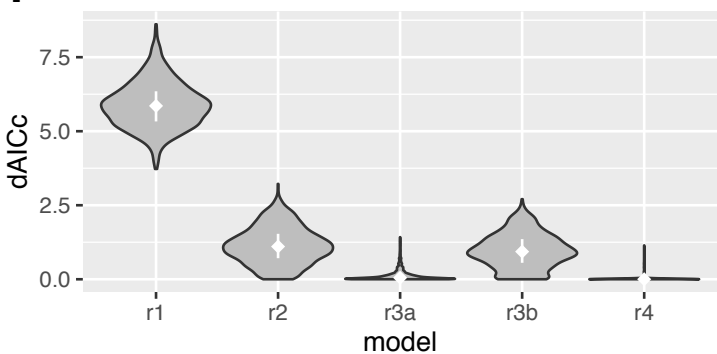
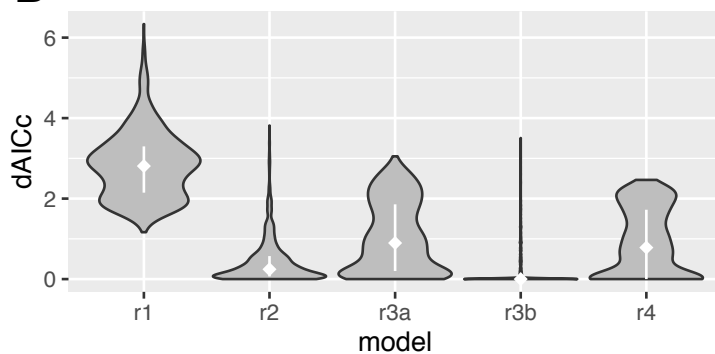
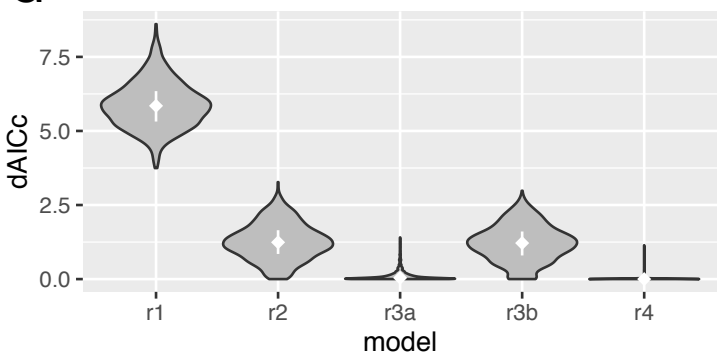
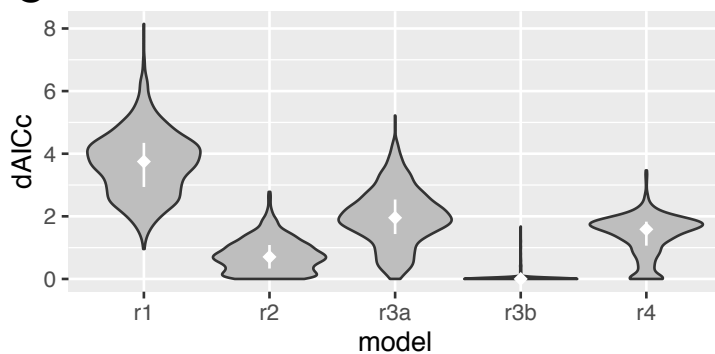
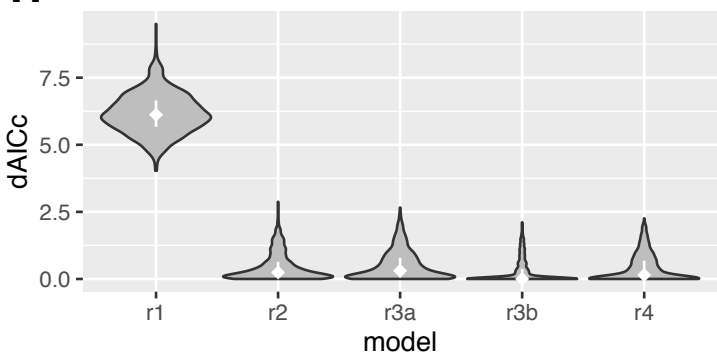
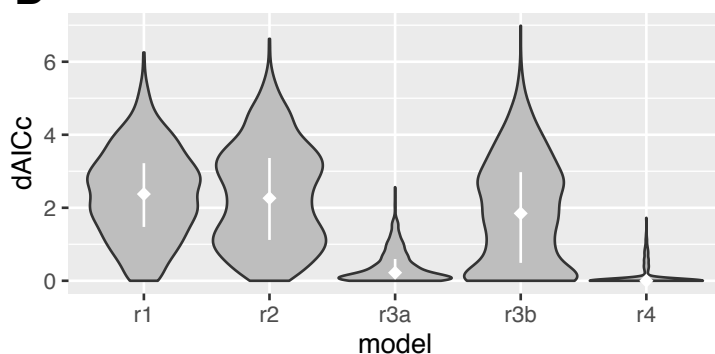
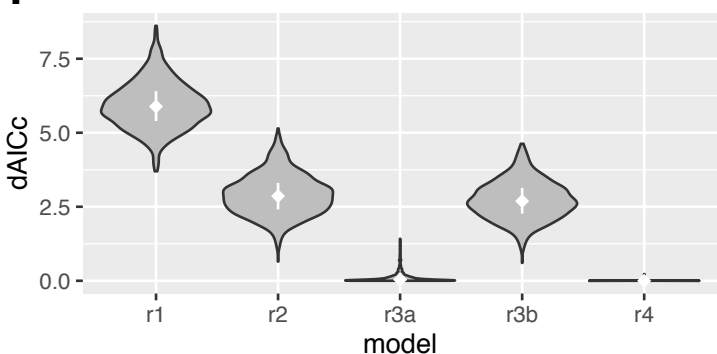
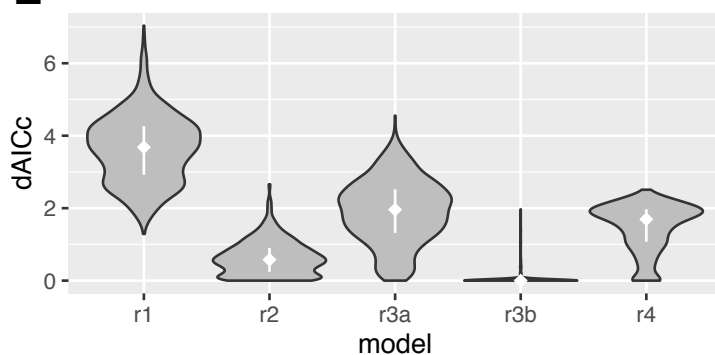
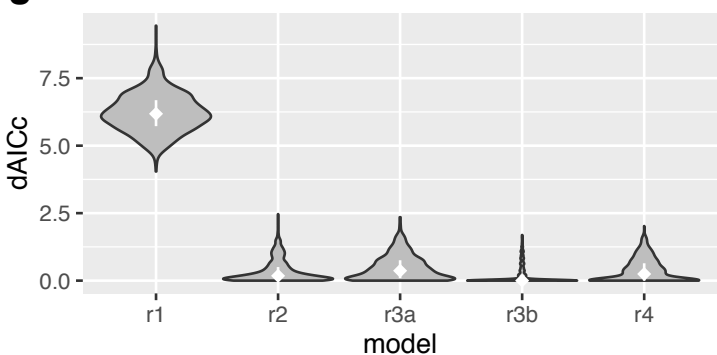
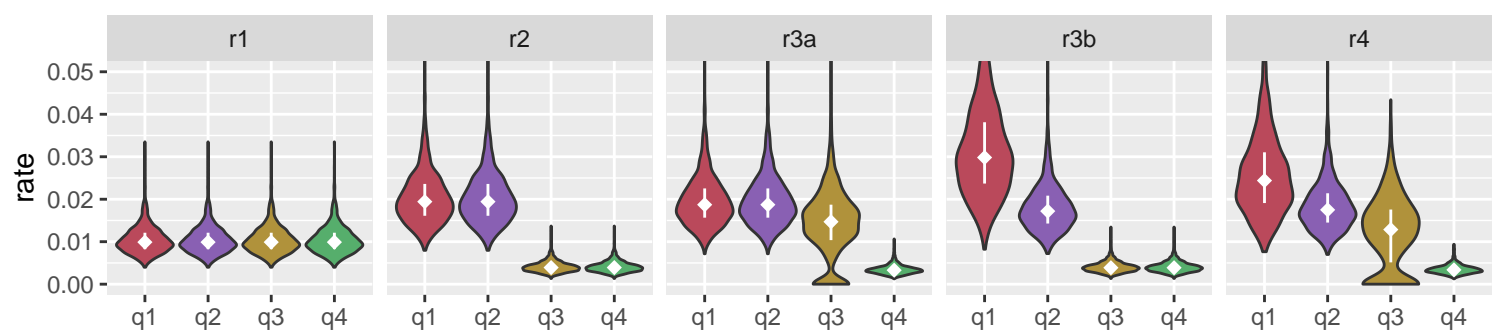
joint**A flat****marginal****F flat****B yang****G yang****C madd****H madd****D con****I con****E flo****J flo**

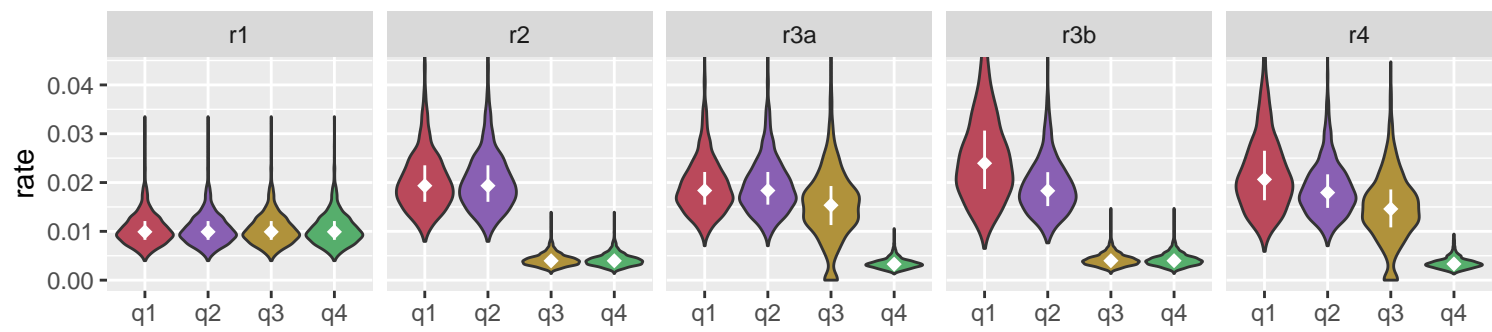
Figure S2. Distribution of transition rates for each model and root probability using joint estimation of transition rates and ancestral states (see main text and Figure 3 for details).

A

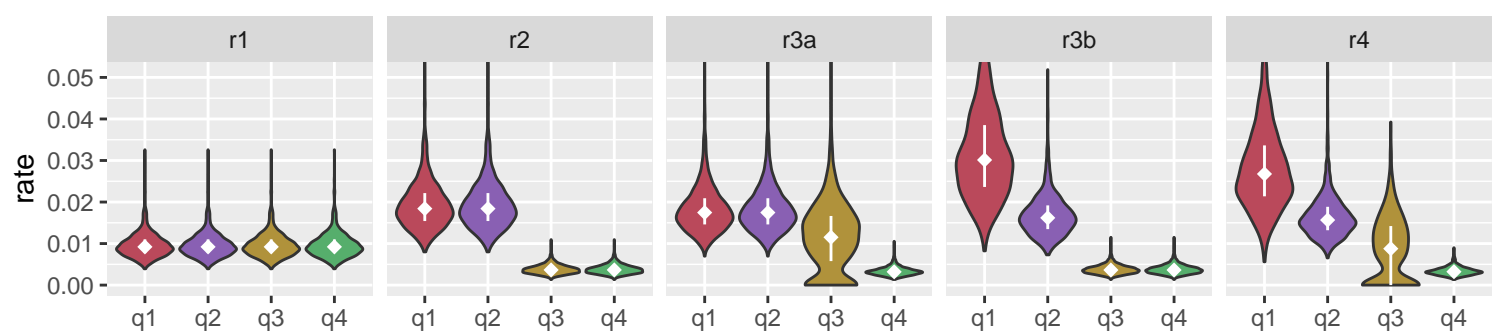
flat

**B**

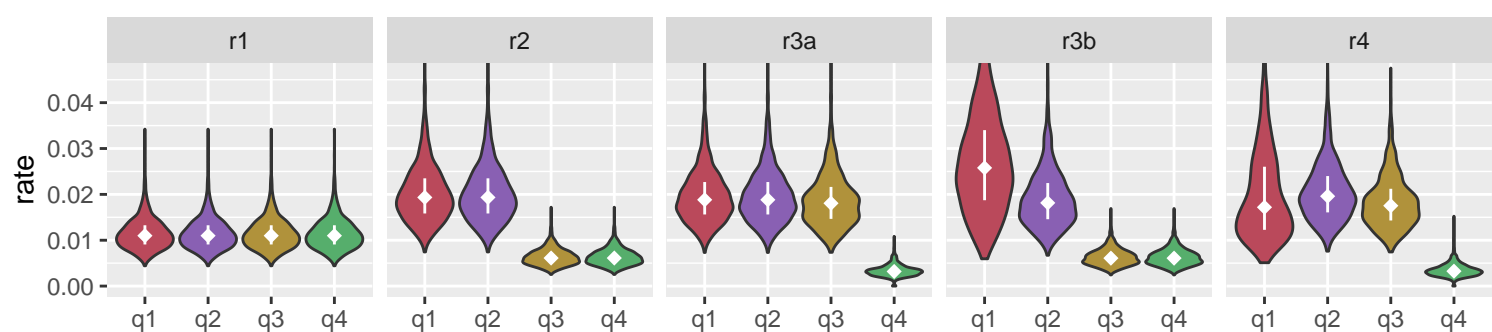
yang

**C**

madd

**D**

con

**E**

flo

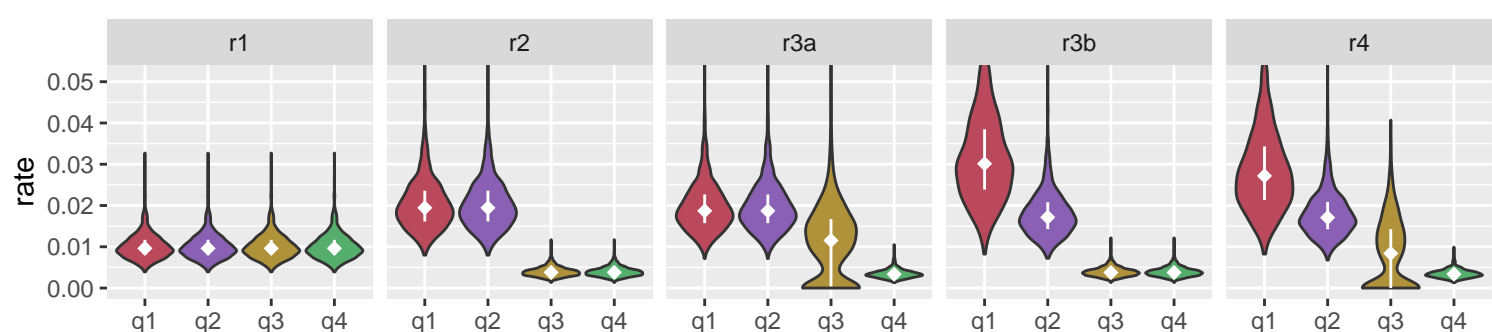
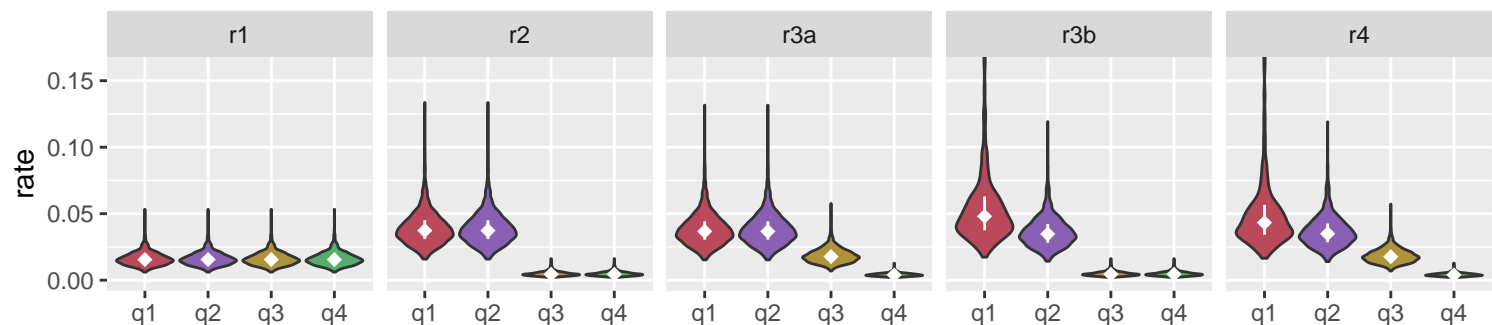


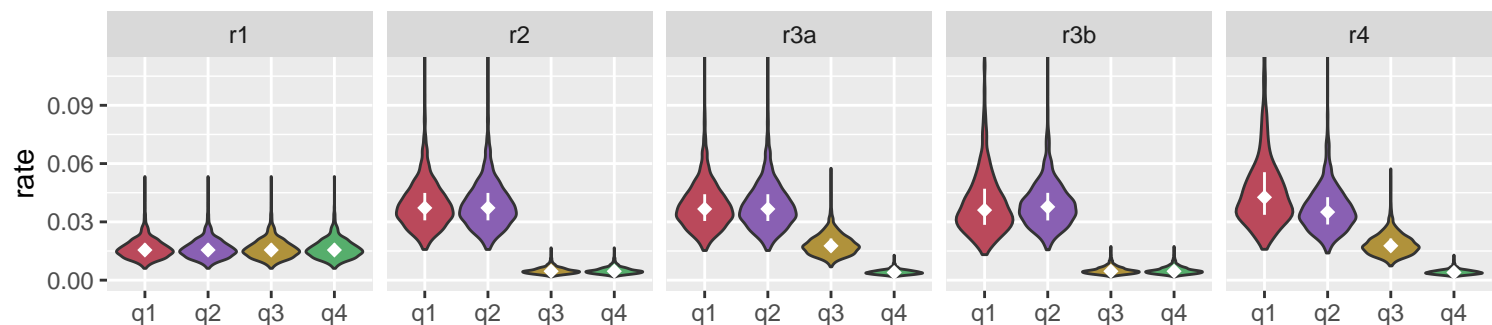
Figure S3. Distribution of transition rates for each model and root probability using marginal estimation of transition rates (see main text and Figure 3 for details).

A

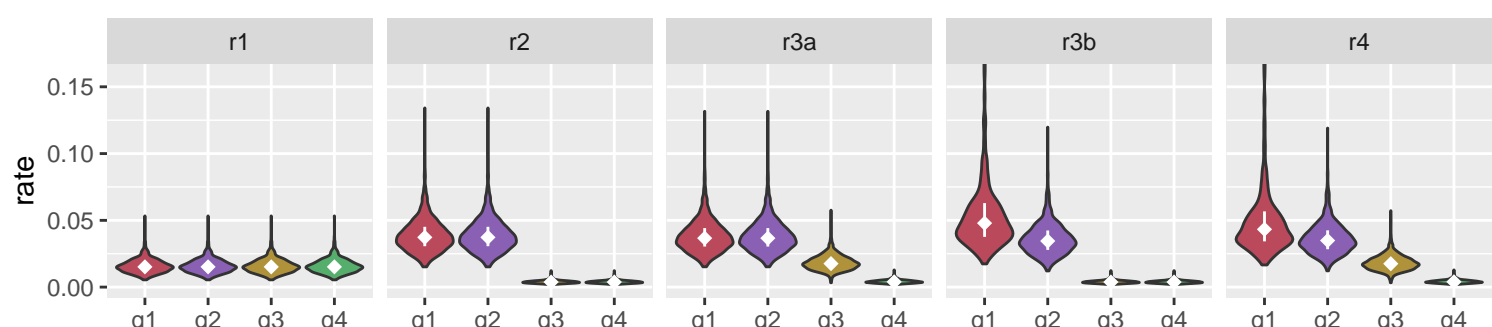
flat

**B**

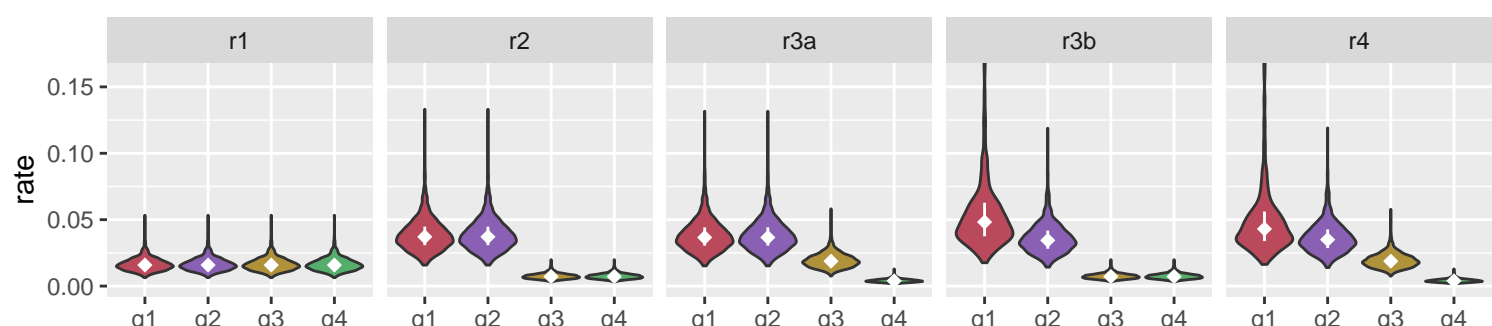
yang

**C**

madd

**D**

con

**E**

flo

